

NISTIR 5809

**Numerical Simulation of Rapid Combustion in an
Underground Enclosure**

Kevin B. McGrattan
Howard R. Baum
Scott P. Deal

April 1996



U.S. Department of Commerce
Michael Kantor, *Secretary*
National Institute of Standards and Technology
Arati Prabhakar, *Director*



Executive Summary

The scenario of interest is a two second firing of a rocket engine in an underground enclosure intended to mimic the effect of burning a high temperature accelerant (HTA). Because of the unusual nature of the problem, at least in the context of typical fire scenarios, two types of numerical models have been applied to the problem. The first, a zone model, divides each room in the enclosure into one or two control volumes, and the transport of mass and energy from the burn room is estimated from the basic conservation laws. The second model, a field model designed for relatively low Mach number flows, solves the conservation equations of mass, momentum and energy discretized over hundreds of thousands of cells. The first approach has the advantage of providing a fast, robust description of the overall thermodynamic quantities of interest. The second approach provides a much more detailed description of the temporal and spatial evolution of these quantities.

The energy release for the two second firing of the rocket is enormous. In all, 245 kg (540 lb) of solid fuel is consumed in two seconds. The total energy released is given as 1093 cal/g (4575 kJ/kg). Of this, it is estimated that about half is lost to the walls or converted to kinetic energy. The remaining energy creates a tremendous pressure and temperature rise throughout the facility. Both the zone model (CFAST2.0) and the field model (NIST Large Eddy Simulation) predict that the pressure in the enclosure after the 2 s firing will rise about 1 atmosphere, and the temperature about 1500 C. Both models simulate one minute following ignition, by which time the pressure in the entire enclosure has returned to atmospheric and the temperature to several hundred degrees over ambient, depending on location. There is little convective motion by this time, and the temperature decrease is largely dependent on the absorption of heat by the walls.

1 Introduction

To assess the impact of a fire involving a high temperature accelerant (HTA) on a relatively small enclosure, it is possible to simulate numerically the transport of combustion products throughout using a variety of computational techniques. However, the difficulty in simulating the effects of a rapid and violent release of heat in one small room is that there are three rather distinct flow regimes which govern the transport of smoke and hot gases from the room throughout the entire enclosure. The first can be characterized as pressure-driven, the second buoyancy-driven, and the third dominated by static heat transfer. During the pressure-driven phase, which in this case lasts only a few seconds, the rapid generation of mass and energy in a small room of the enclosure increases the pressure in the room to nearly twice the atmospheric pressure, driving the hot gases out at speeds approaching sonic. The fact that the enclosure is underground and vented only through a small opening to the atmosphere enhances the effect of the pressure. After the source of heat is removed, however, the pressure in the burn room and the overall enclosure quickly equilibrate at which point the flow becomes dominated by the buoyancy-induced motion of the hot gases spreading throughout the enclosure and creating a stratified temperature distribution. This second phase lasts on the order of a minute. Following this, there is little convective motion, and heat is gradually absorbed by the walls and lost through the vent.

While it is possible to numerically simulate the entire experiment by directly solving the full set of Navier-Stokes equations for a compressible fluid with the inclusion of heat transfer and thermal radiation, this would require a large amount of computational resources, most of which would be devoted to resolving the extremely high speed, high temperature flow out of the rocket nozzle. The spatial resolution for such a calculation would be extremely limited. However, the numerical simulation of the less violent, buoyancy-driven flow regime could be greatly enhanced by taking advantage of the relatively low speeds and modest temperatures. Typically room fire simulations are of this type, and a numerical model has been developed at NIST to solve the relevant flow equations [3]. The technique is referred to as a large eddy simulation (LES). The term “large eddy” refers to fluid motion on length scales which are about two orders of magnitude smaller than the overall enclosure length. To achieve this type of resolution means that the enclosure must be discretized into roughly one million cells, each of which can be thought of as a control volume in which mass, momentum and energy are conserved. Of course, this requires a fairly powerful computer to implement; but because of the specialized nature of the algorithm, it demands far less than would be expected. In fact, these types of simulations are currently performed on desktop workstations rather than on supercomputers as was the practice only a few years ago.

The way to achieve such performance is to balance all aspects of the problem so that high accuracy in one area is not negated by low accuracy in another. Specifically, reasonable approximations can be made about the rocket engine so as to enable the computation of the flow over a fairly long time period. This would be very difficult, if not impossible, if details of the high speed flow out of the rocket nozzle were desired in addition to the long term effect on the entire enclosure. Thus, the approach taken is to distribute the energy release of the rocket throughout the entire burn room, making the assumption that the violent firing of the rocket creates a well-mixed zone whose average pressure and temperature can be easily calculated. This mimics the approach taken by a so-called “zone model”, where the enclosure

is divided up into a few control volumes (one of which is the burn room) in which mass and energy conservation are enforced. Indeed, a zone model (CFAST2.0 [1]) has been applied to the problem as a check on the results of the more sophisticated large eddy simulation. Because the problem is highly unusual, using the zone model to check global quantities has greatly increased the confidence in the numerical results.

2 Problem Description

The floor plan of the underground test structure is shown in Fig. 1. The experiment is to consist of the firing of a rocket engine in the room designated R1 (top, left). For the numerical modeling to be discussed here, the details of the rocket engine are not necessary. The only information required is the total amount of fuel consumed and the total energy release. The rocket engine is to be fired for 2 seconds during which time it is estimated that 245 kg (540 lb) of fuel will be consumed. It is estimated that the total energy content of the fuel is 1093 calories per gram, of which 646 cal/g is converted into kinetic energy and 447 cal/g into the internal energy of the rocket exhaust. The goal of the numerical simulation is to predict the temperatures and pressures to be expected throughout the enclosure for the first minute of the test. Two approaches are taken. The first is a zone model, CFAST2.0 [1], which will be described in the next section. Next, a field model, the NIST Large Eddy Simulation, is applied to the problem. This second model is used internally at NIST on a variety of problems, but is not yet available externally.

3 Zone Modeling of the Pressure-Driven Flow

Following is a basic description of zone models, together with the results of one used widely by the fire research community, CFAST2.0. A zone model as applied to typical enclosure fires assumes that each room or compartment may be divided into two distinct zones, a hot upper layer and a cold lower layer. Each zone is characterized by an average temperature, and conservation equations of mass and energy dictate the movement of the hot gases from zone to zone and room to room. This approach is applied to multi-room enclosures to estimate the rate at which the smoke spreads and the average temperatures one might expect to find in each room.

The simplest approach to the scenario described above is to consider the underground facility shown in Fig. 1 as two compartments – the burn room and all the other rooms combined. Also, during the firing of the rocket and shortly thereafter, each compartment may be characterized as a single zone with a single averaged temperature and pressure. For this simple description, a mass and energy conservation equation may be applied to each “room”, resulting in the following four ordinary differential equations for the pressure and density of each:

Burn room mass conservation

$$V_r \frac{d\rho_r}{dt} = \dot{m} - C_0 \rho_r A_E \sqrt{\frac{2(P_r - P_e)}{\rho_r}} \quad (1)$$

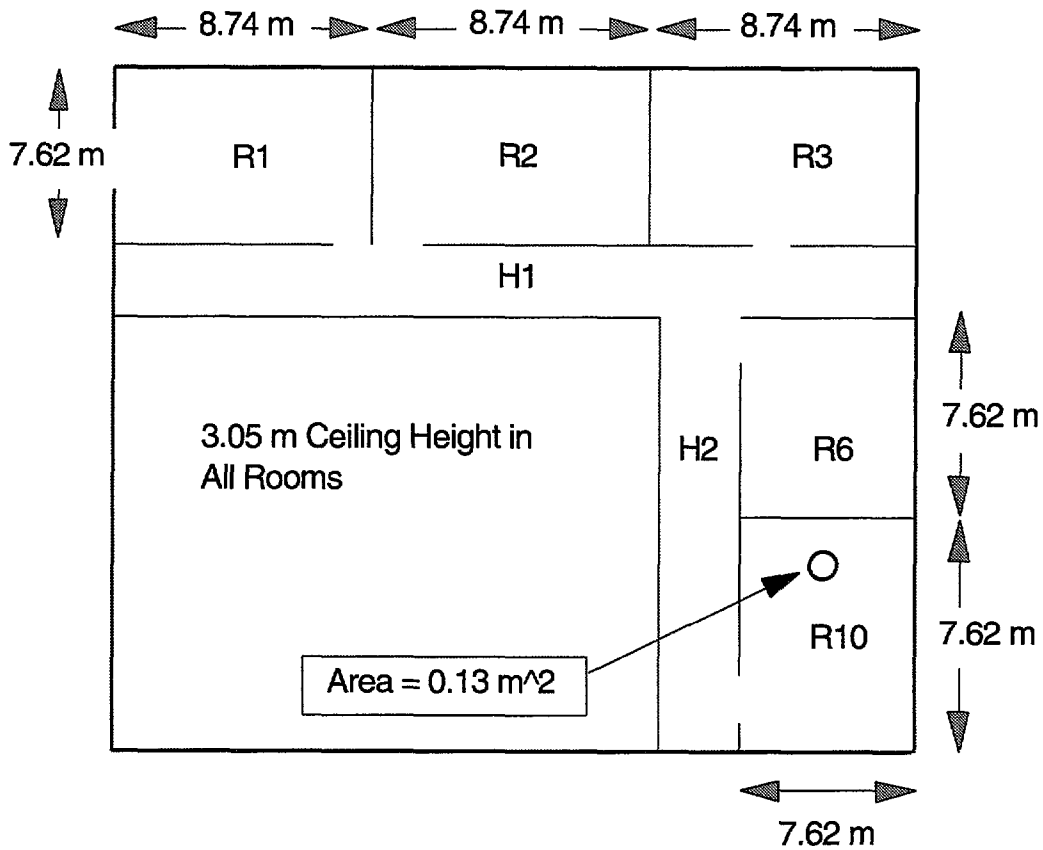


Figure 1: Floor plan of the underground facility. All dimensions are in meters. The height of the rooms is 3.05 m (10 ft). The walls appear to have negligible width but in reality are 0.46 m thick between rooms and 0.76 m thick at exterior walls. Below Rooms R6 and R10 are similarly sized rooms connected via a stairway in hallway H2. Room R10 and the two downstairs rooms are all connected, and vented to the atmosphere through a vertical vent approximately 35 cm in diameter. It is assumed that this is the only ventilation from the enclosure to the atmosphere. The area in the lower left hand side of the figure is sealed off and assumed to play no part in the scenario outlined here.

Zone Model Simulation Parameters	
h_N	4575 kJ/kg (1093 cal/g)
β	see discussion below
\dot{m}	123 kg/s (270 lb/s)
V_e	1550 m ³ (54740 ft ³)
V_r	203 m ³ (7170 ft ³)
A_E	1.95 m ² (21 ft ²)
A_V	0.13 m ² (1.4 ft ²)
γ	1.4
C_0	0.70
ρ_0	1.226 kg/m ³ (0.076 lb/ft ³)
P_0	101.3 kPa (1 atm)

Table 1: **Parameters used in the CFAST2.0 modeling simulation of the rocket firing.**

Enclosure mass conservation

$$V_e \frac{d\rho_e}{dt} = C_0 \rho_r A_E \sqrt{\frac{2(P_r - P_e)}{\rho_r}} - C_0 \rho_e A_V \sqrt{\frac{2(P_e - P_0)}{\rho_e}} \quad (2)$$

Burn room mass and energy conservation

$$\frac{V_r}{\gamma - 1} \frac{dP_r}{dt} + \frac{\gamma}{\gamma - 1} C_0 P_r A_E \sqrt{\frac{2(P_r - P_e)}{\rho_r}} = (1 - \beta) h_N \dot{m} \quad (3)$$

Enclosure mass and energy conservation

$$\frac{V_e}{\gamma - 1} \frac{dP_e}{dt} + \frac{\gamma}{\gamma - 1} C_0 P_e \left[A_V \sqrt{\frac{2(P_e - P_0)}{\rho_e}} - A_E \sqrt{\frac{2(P_r - P_e)}{\rho_r}} \right] = 0 \quad (4)$$

Here V is volume, A is area, ρ density, P pressure, \dot{m} mass flux from the engine, h_N the total energy content of the fuel (the exit sensible enthalpy of the rocket exhaust), and β the fraction of the sensible enthalpy converted to kinetic energy, lost to the walls, radiation, *etc.* The orifice coefficient C_0 is the fraction of the total potential mass flux through a doorway or vent due to a pressure differential. The subscript “ r ” refers to the burn room, “ e ” the other compartments of the enclosure combined, “ E ” the doorway between the burn room and the other compartments, “ V ” the vent, and “ 0 ” the atmosphere outside. The parameters used to simulate the first couple of seconds of the experiment are listed in Table 1.

In addition to the basic conservation equations described above, CFAST2.0 contains additional routines to estimate heat transfer to walls, oxygen depletion, *etc.* Most of these features apply to more typical fire growth problems and do not apply to the problem at hand. Only heat transfer to walls has been retained. The largest uncertainty in prescribing input parameters for the model is in estimating the heat release rate of the fuel. The energy

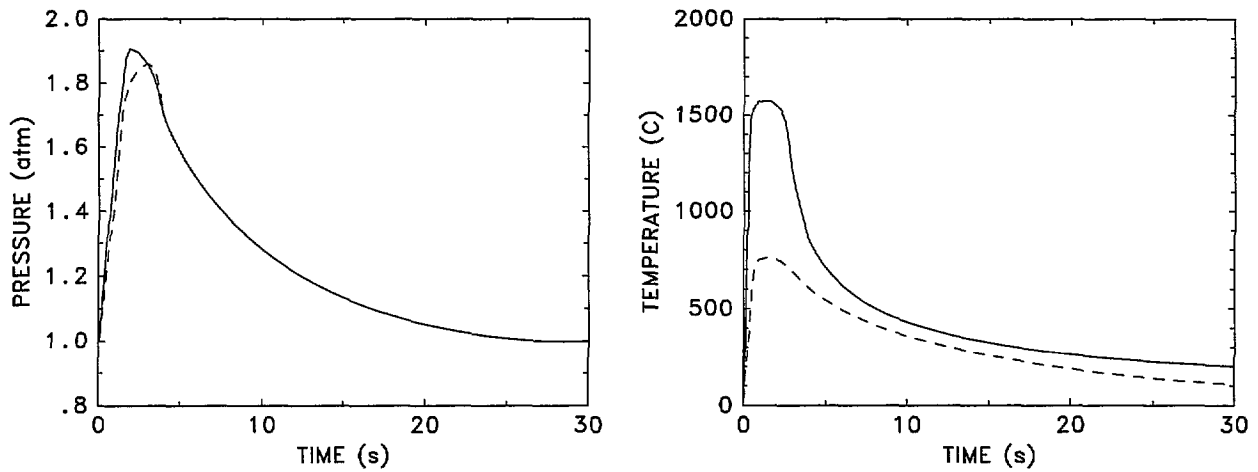


Figure 2: CFAST2.0 predicted average pressure and temperature for the burn room (solid line) and the rest of the enclosure (dashed line).

from the rocket fuel (1093 cal/g) is broken down as kinetic energy of the jet exiting the nozzle (646 cal/g) and as internal energy of the hot gas exhaust (447 cal/g). These figures are derived either from calculations or from actual temperature and velocity measurements at the nozzle. In any event, they depend on the specific type of rocket engine used. As far as the zone model is concerned, the kinetic energy of the rocket exhaust at the nozzle is not included in the estimate of the heat release rate of the fuel — the kinetic energy is accounted for by the assumption that the gases are well-mixed. However, a certain fraction of the kinetic energy is recovered as thermal or internal energy as the jet impinges on the walls of the burn room; some of the kinetic energy is converted to mechanical energy which is absorbed by the wall; and finally most of the kinetic energy remains as kinetic energy. Of importance here is the fraction converted back to internal energy, which is estimated to be about 25%.

After adjusting the heat release rate of the fuel, the calculation estimates that the pressure in the burn room rises to about 1.9 atmospheres in 2 seconds, at which time the rocket engine is turned off and the pressure in the burn room quickly equilibrates with that of the rest of the enclosure. Gradually, the pressure will decrease to ambient due to the venting to the atmosphere and heat loss to the boundaries, but this will take place over several tens of seconds due to the small cross section of the vent (roughly 40 cm (16 in) in diameter). The average temperature in the burn room rises to about 1500 C (2730 F) in 2 seconds, while the average upper layer temperature in the rest of the enclosure rises to about 750 C (1400 F). After the engine is turned off and the pressure equilibrates, the flow becomes buoyancy rather than pressure driven, and the hot gases begin to stratify. The hot gases from the burn room spread throughout the entire enclosure, forming a hot upper layer and a relatively cool lower layer. During this period, which will last tens of seconds, the flow is dominated by buoyant convection. After several minutes, the temperature in the burn room approaches the average temperature of the enclosure, at which time the flow is dominated by heat loss to the boundaries. Results of the model for the scenario described above are summarized in Fig. 2.

4 Field Modeling of the Buoyancy-Driven Flow

The limitation of the zone model is that it only predicts average temperatures over large volumes. For a more detailed description of the flow, the actual equations of motion must be solved in some approximate form. Consider an ideal gas with constant eddy viscosity and thermal conductivity driven by a prescribed heat source. The motion of the fluid is governed by the conservation equations of mass, momentum and energy, plus an equation of state relating the thermodynamic quantities

$$\frac{\partial \rho}{\partial t} + \nabla \cdot \rho \mathbf{u} = 0 \quad (5)$$

$$\rho \left(\frac{\partial \mathbf{u}}{\partial t} + \mathbf{u} \cdot \nabla \mathbf{u} \right) + \nabla p - \rho \mathbf{g} = \mu \left(\frac{4}{3} \nabla \nabla \cdot \mathbf{u} - \nabla \times \boldsymbol{\omega} \right) \quad (6)$$

$$\rho c_p \left(\frac{\partial T}{\partial t} + \mathbf{u} \cdot \nabla T \right) - \left(\frac{dp}{dt} + \mathbf{u} \cdot \nabla p \right) = \dot{q} + \nabla \cdot k \nabla T \quad (7)$$

$$p = \mathcal{R} \rho T \quad (8)$$

Here, all symbols have their usual fluid dynamical meaning: ρ is the density, \mathbf{u} the velocity vector, p the pressure, \mathbf{g} the gravity vector, μ the dynamic viscosity, c_p the constant-pressure specific heat, T the temperature, k the thermal conductivity, t the time, \dot{q} the prescribed rate of heat release, and \mathcal{R} the gas constant equal to the difference of the specific heats $\mathcal{R} = c_p - c_v$

Application of these equations to the problem of buoyant convection from thermal sources has been performed by Rehm and Baum [2]. The essential piece of the analysis concerns the decomposition of the pressure into an average background component, a hydrostatic component and a thermally-induced perturbation. Sound waves are filtered out of the problem by replacing the pressure in Eq. (7) with the background pressure, which is solely a function of time. The energy and state equations are thus rewritten

$$\rho c_p \left(\frac{\partial T}{\partial t} + \mathbf{u} \cdot \nabla T \right) - \frac{dp_0}{dt} = \dot{q} + \nabla \cdot k \nabla T \quad (9)$$

$$p_0(t) = \rho \mathcal{R} T \quad (10)$$

Mathematically, this modification adds an elliptic character to the system of partial differential equations. This fact is exploited in the calculations after the period of intense heat addition is over because the rate at which time steps may be taken will not be inhibited by the sound speed, as they are for the unmodified Navier-Stokes equations. In fact, this modified form of the Navier-Stokes equations has been termed ‘‘thermally expandable’’ to emphasize that even though the fluid is compressible, the pressure is not the driving force but rather the buoyancy.

As one might expect, therefore, the divergence of the flow $\nabla \cdot \mathbf{u}$ is a very important quantity in the analysis to follow, and it is readily found by combining Eqs. (5) and (9) and using the equation of state (10)

$$p_0 \nabla \cdot \mathbf{u} + \frac{1}{\gamma} \frac{dp_0}{dt} = \frac{\gamma - 1}{\gamma} (\dot{q} + \nabla \cdot k \nabla T) \quad (11)$$

where $\gamma = c_p/c_v$. Integrating Eq. (11) over the entire domain Ω yields a consistency condition for the background pressure $p_0(t)$

$$p_0 \int_{\partial\Omega} \mathbf{u} \cdot d\mathbf{S} + \frac{V}{\gamma} \frac{dp_0}{dt} = \frac{\gamma - 1}{\gamma} \left(\int_{\Omega} \dot{q} dV + \int_{\partial\Omega} k \nabla T \cdot d\mathbf{S} \right) \quad (12)$$

where V is the volume of the enclosure. Notice that this equation expresses the fact that the enclosure pressure is increased by the addition or subtraction of heat and mass.

The background pressure can be expressed in terms of a spatially averaged temperature $T_0(t)$ and density $\rho_0(t)$

$$p_0 = \mathcal{R} \rho_0 T_0 \quad (13)$$

Perturbations to each are represented by the relations

$$T = T_0(t)(1 + \hat{T}) \quad ; \quad \rho = \rho_0(t)(1 + \hat{\rho}) \quad (14)$$

Now, if the background processes are taken as adiabatic, *i.e.*

$$\frac{\rho_0}{\rho_\infty} = \left(\frac{p_0}{p_\infty} \right)^{1/\gamma} \quad (15)$$

then the energy equation can be expressed in terms of the perturbation temperature \hat{T} and the divergence

$$\frac{\partial \hat{T}}{\partial t} + \mathbf{u} \cdot \nabla \hat{T} = (1 + \hat{T}) \left[\nabla \cdot \mathbf{u} + \frac{1}{\gamma p_0} \frac{dp_0}{dt} \right] \quad (16)$$

The background pressure is found from Eq. (12). Mass loss through doors and windows can be treated in several ways. For small vents, the velocity flux can be expressed in terms of the background pressure and density, much like in the zone model formulation above

$$\int_{\partial\Omega} \mathbf{u} \cdot d\mathbf{S} = \begin{cases} A c_0 \sqrt{\frac{2(p_0 - p_\infty)}{\rho_0}} & (p_0 > p_\infty) \\ A c_0 \sqrt{\frac{2(p_\infty - p_0)}{\rho_\infty}} & (p_0 < p_\infty) \end{cases} \quad (17)$$

where A is the area of the vent and c_0 is an orifice coefficient usually taken in the range $\pi/(\pi + 2) \approx 0.61 \leq c_0 \leq 0.7$ [5].

The pressure is decomposed into three components, the background $p_0(t)$, the hydrostatic, and a perturbation to the hydrostatic \hat{p}

$$p(\mathbf{r}, t) = p_0(t) - \rho_0(t)gz + \hat{p}(\mathbf{r}, t) \quad (18)$$

where z is the vertical spatial component. The hydrostatic pressure is eliminated from the momentum equation by combining it with the buoyancy term. Also the term $|\mathbf{u}|^2/2$ is combined with the term \hat{p}/ρ_0 to form a total pressure, \hat{p} . The constant dynamic viscosity μ divided by the density ρ is taken as a constant kinematic viscosity coefficient ν . The system of equations that are to be solved numerically is

$$\frac{\partial \mathbf{u}}{\partial t} - \mathbf{u} \times \boldsymbol{\omega} + \nabla \hat{p} - \hat{T} \mathbf{g} = \nu \left(\frac{4}{3} \nabla \nabla \cdot \mathbf{u} - \nabla \times \boldsymbol{\omega} \right) \quad (19)$$

$$\frac{\partial \hat{T}}{\partial t} + \mathbf{u} \cdot \nabla \hat{T} = (1 + \hat{T}) \left[\nabla \cdot \mathbf{u} + \frac{1}{\gamma p_0} \frac{dp_0}{dt} \right] \quad (20)$$

$$p_0 \int_{\partial\Omega} \mathbf{u} \cdot d\mathbf{S} + \frac{V}{\gamma} \frac{dp_0}{dt} = \frac{\gamma - 1}{\gamma} \left(\int_{\Omega} \dot{q} dV + \int_{\partial\Omega} k \nabla T \cdot d\mathbf{S} \right) \quad (21)$$

To obtain the pressure perturbation, take the divergence of the momentum equation

$$\frac{\partial \nabla \cdot \mathbf{u}}{\partial t} + \nabla \cdot \mathbf{F} + \nabla^2 \hat{p} = 0 \quad (22)$$

where all the convective and diffusive terms have been incorporated in the term \mathbf{F} . This equation is solved with a fast Poisson solver.

The numerical techniques for solving equations of this form may be found in Reference [3]. Briefly, the equations are a mixed parabolic/elliptic system of partial differential equations: *i.e.*, the equations for the temperature and for the velocity components are parabolic, whereas that for the pressure is elliptic. The equations which govern low Mach number flow are well known to have this mixed character. Analytical studies of the ability of several candidate finite difference schemes to calculate internal gravity waves without dissipation led to the conclusion that methods of second order accuracy in space and time are highly desirable for systems of this type [4]. A simple Runge-Kutta second order scheme is used — all spatial derivatives are approximated by second order central differences and the flow variables are updated in time following a simple predictor-corrector explicit method. The grid is taken to be uniform in the coordinate directions although the spacings in each direction may be different.

To simplify the calculation, some additional approximations were implemented. First, it was assumed that the rooms downstairs of the main floor served only as a reservoir for the pressure build-up. Specifically, the overall enclosure volume V in Eq. (12) was taken to be that of the actual underground facility, even though the computational domain consisted only of the compartments on the main floor. The main reason for this approximation is that the fast Poisson solver used in the problem uses Fast Fourier Transforms (FFT) in two spatial directions, and works most efficiently for rectangular, uniformly-gridded problems.¹ To include the downstairs compartments would have enormously increased the size of the computational problem without delivering any important changes to the conclusions drawn.

A similar approximation technique was used at the inflow and outflow vents. To simulate the addition of mass and energy from the rocket motor, a large vent was opened up on the floor of the burn room. Hot gas was pushed in through the vent so as to mimic the mass and energy release of the motor, but not the high velocities for which the methodology employed here is not suited. Similarly, the small exit vent was simulated with a larger opening which vented an equivalent loss of mass. This mass loss was based on the orifice formulae given in Eq. (17). In the case of both the inflow and outflow vents, it is not the objective of the study to simulate exactly the dynamics of the flow at the nozzle of the rocket motor nor at the exit vent. Indeed, given the size of the entire enclosure, it is impossible with the available computational resources to adequately resolve the flow in these regions while simultaneously

¹The uniform gridding of the computational domain is required in two spatial directions, the third direction may be non-uniformly gridded to cluster cells where most of the action is.

simulating the flow in the entire facility. Rather, the objective of the computation is to predict the overall transfer of energy from the burn room throughout the entire enclosure.

The greatest uncertainty in a simulation of a fire or some other large thermal source is determining the heat release rate, as well as the exchange of energy between internal, kinetic, mechanical and radiative forms. For the problem at hand, an estimated 540 lb (245 kg) of fuel is to be consumed in 2 s. The energy content of the fuel is estimated to be 1,093 cal/g, and it is estimated that roughly 60% of this will be converted to kinetic energy by the rocket motor, 40% to internal energy of the gas. For both the zone and field models employed in this study, however, this breakdown of the total enthalpy into parts is not relevant because neither model is designed to predict the behavior of the near sonic velocities of gases emanating from the motor, nor the impact of the jet on the wall of the burn room. In fact, given the ideal assumptions of most fluid models, it is unlikely that any could truly describe the exchange of energy taking place in or near the motor. Instead an estimate must be made of the fraction of the total enthalpy which characterizes the burning. Typically for a fire, it is assumed that about 30% of the heat released is lost to thermal radiation. Some of this radiative energy is reabsorbed by the gas, some by the walls. For the rocket motor, much of the total energy is converted into the kinetic energy of a high speed jet impinging on a concrete wall. It is very difficult to predict how much of that energy remains kinetic and how much is converted back to internal energy or absorbed by the wall. Given all of these uncertainties, it will be assumed that about half of the total energy is lost in the burn room in the first few seconds due to the absorption by the walls of internal and kinetic energy.

As discussed above, the energy is introduced into the problem by pumping hot gas into the burn room through a large vent at a modest velocity. The temperature and velocity of the gas depends on two quantities: the mass flux rate and the effective enthalpy. Assuming that 245 kg of fuel is gasified in 2 s, the mass flux rate \dot{m} is taken as 122.5 kg/s. The effective enthalpy is assumed to be 500 cal/g (2090 J/g), from which the temperature of the gas can be estimated from

$$\int_{T_\infty}^T c_p d\tau \approx 2.1 \times 10^6 \text{ J/kg} \quad (23)$$

Then the exit velocity u_e can be found from

$$\rho_e u_e A_v = 122.5 \text{ kg/s} \quad (24)$$

where ρ_e is the density of the gas (found from the temperature) and A_v is the area of the vent. The exit velocity of the gas is about 30 m/s, about a tenth of the sonic speed.

The calculation simulates 60 seconds of the experiment, starting just as the rocket motor is switched on. The calculation requires about 75 hours on an IBM RISC/6000 workstation, with over half of that time devoted to the 2 seconds during which the rocket was firing. The underground enclosure is discretized into 524,288 uniformly spaced cells (128 in both horizontal directions and 32 in the vertical). The dimensions of an individual cell are 21 cm by 21 cm by 9.5 cm. The temperature, velocity and pressure of the air in each cell is stored periodically for analysis. Also, particles are introduced through the hot gas vent and tracked so as to provide an animation of the simulation.

Because the calculation is time-dependent and there are three spatial coordinates, it is difficult to present all the results in a simple way. Temperature data is saved periodically dur-

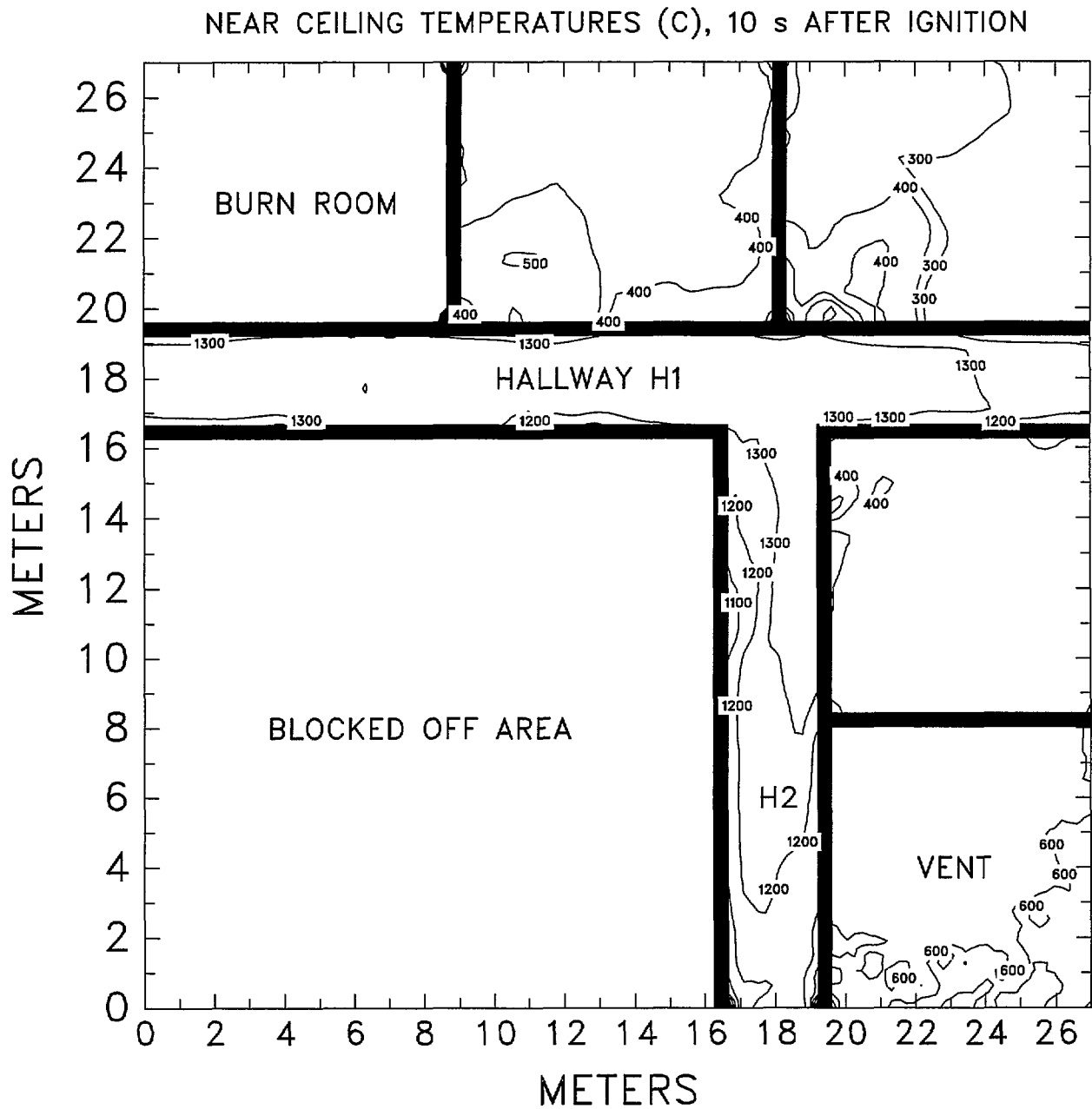


Figure 3: LES predicted temperatures (C) approximately 30 cm (1 ft) from the ceiling 10 s after ignition. Note the difference in temperature between the hallways and the rooms other than the burn room. Doorways are not shown, but rather the soffit above the doorways which contain much of the hot gas in the hallways.

ing the calculation, from which two-dimensional slices can be taken and contoured. Fig. (3) shows the ceiling temperatures 10 s after ignition. Notice that the rooms that are not vented do not heat up nearly as much as the hallways because the hot gases in the upper layer are blocked by the soffits above the doorways. The temperatures in the two hallways H1 and H2 are shown at various times during the calculation. Fig. 4 shows the temperature profiles in hallway H1 every 10 seconds following ignition of the rocket engine. The stratification of the hot gases emanating from the burn room (left) is evident from the contour plots, with temperatures ranging from about 200 C near the floor to about 1400 C near the ceiling. This stratification also defines the movement of the air from the burn room along the ceiling towards the exit vent, with cooler air moving near the floor in the opposite direction. This bi-directional flow persists until the average enclosure pressure returns to atmospheric after about 40 s. At this point, the air is relatively calm, and the temperature gradually decreases as heat is lost to the walls. Most of the hotter gases from the burn room are confined to the hallways since the soffits above the compartment doorways impede much of the smoke and hot gases from entering. Once the hot layer in the hallway grows thicker than the soffit height, then the hot gases spill over into the individual rooms.

Fig. 5 shows the temperature profiles in the hallway H2. The temperatures here vary from about 100 C to about 800 C. Once the smoke and hot gases reach the end of the hallway H2, the hot layer begins to thicken. Temperatures in this layer vary between 200 C to about 400 C, and this gradually decreases as the heat is lost to the boundaries and to the vent. It is clear from the figure that the temperature in the room R2 is significantly less than that of the hallway due to the protection provided by the soffit above the door and the fact that most of the hot gases from the burn room flow towards the exit vent.

5 Conclusions

The scenario described in this paper stretches the limit of modern numerical fire prediction techniques, both the zone models and the field models. An event as violent and rapid as the firing of a rocket in a small underground enclosure is not usually considered a typical fire scenario due to the extremely high pressures and velocities generated. Like most interesting physical problems, understanding of all processes cannot be gained through one experiment or one numerical model, but rather through a variety of techniques which try to divide the problem into manageable parts. For the problem described here, no one numerical model can satisfactorily describe all aspects of the problem. Nevertheless, a combination of techniques has been used to describe many aspects of the event, but certainly not all. The initial violent firing of the rocket is described only in terms of averaged quantities in the burn room during the first few seconds of the experiment. After that, the field model describes the movement of heat and combustion products throughout the enclosure at a spatial resolution which of about 23 cm. This high resolution is important when describing the mixing of the hot gases emanating from the burn room with the cooler gases outside.

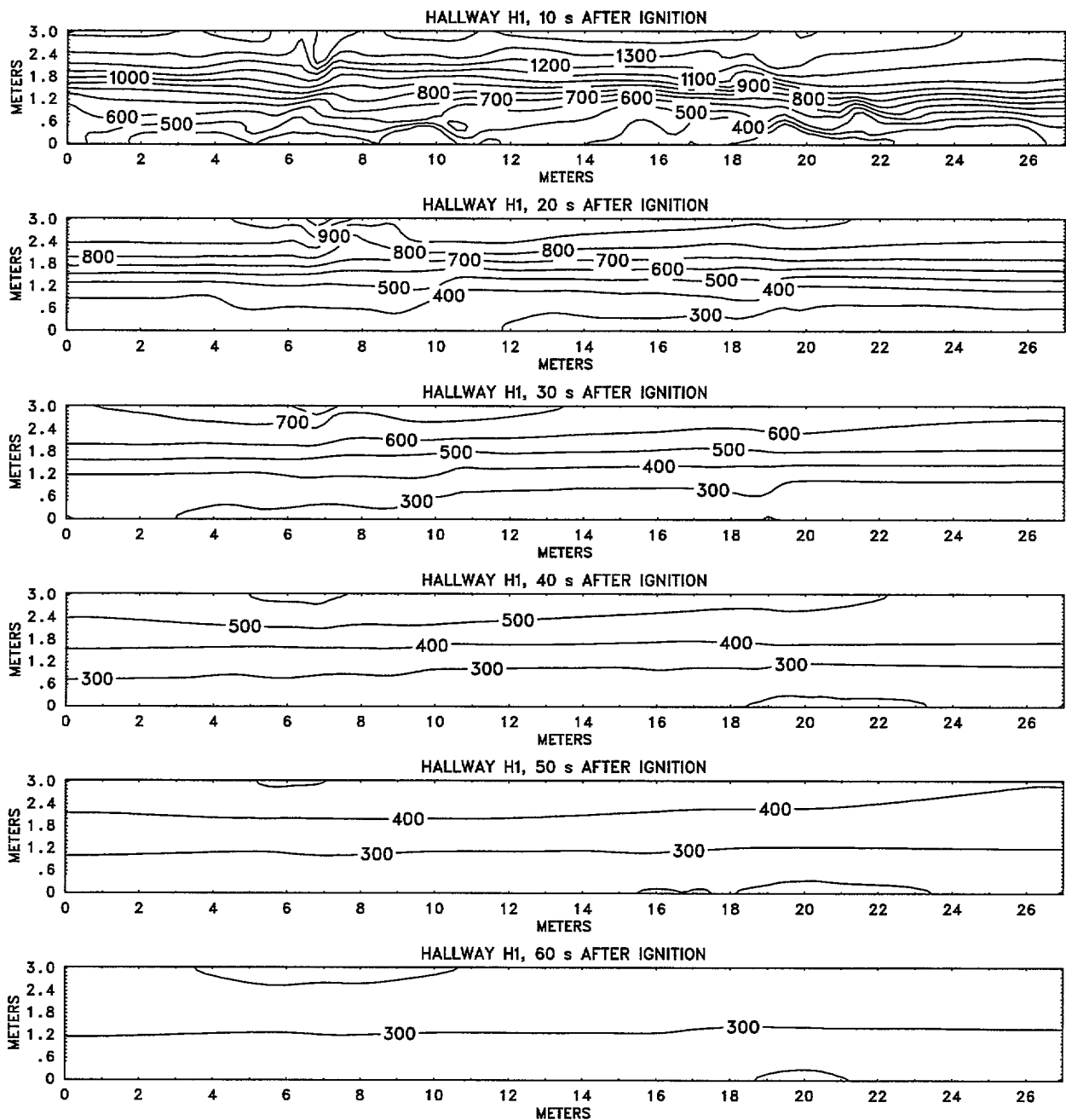


Figure 4: Temperature profiles in the hallway H1 at increments of 10 seconds following the ignition of the rocket engine. The burn room is to the left side in the figures.

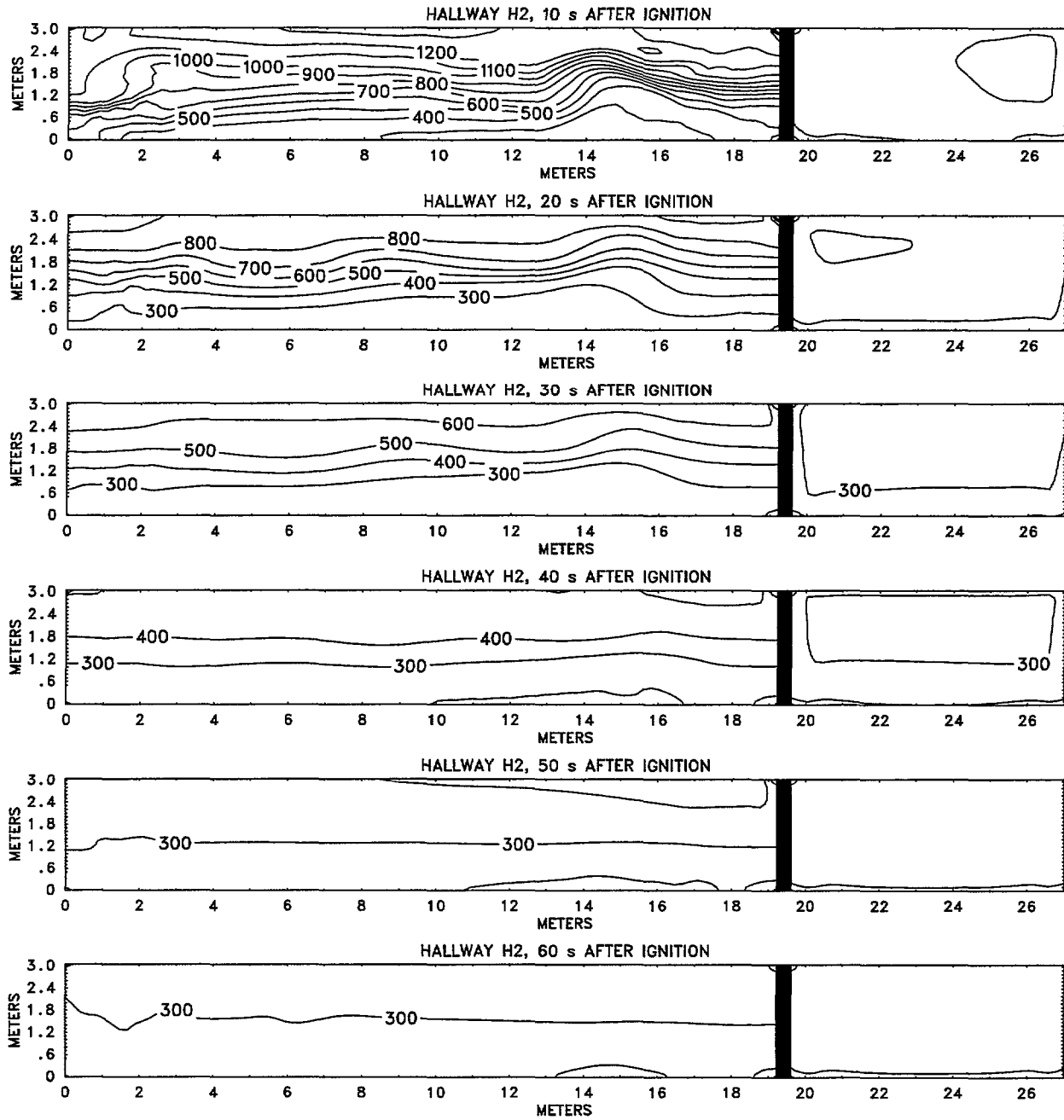


Figure 5: Temperature profiles in the hallway H2 at increments of 10 seconds from the ignition of the rocket engine. The solid black line indicates the wall separating hallway H1 from room R2.

References

- [1] Peacock, R.D., Forney, G.P., Reneke, P., Portier, R., Jones, W.W., "CFAST, the Consolidated Model of Fire Growth and Smoke Transport," NIST Technical Note 1299, National Institute of Standards and Technology, Gaithersburg, MD 20899, February, 1993.
- [2] Rehm, R.G. and H.R. Baum, "The Equations of Motion for Thermally Driven, Buoyant Flows", *Journal of Research of the NBS.* 83, pp. 297-308, May-June 1978.
- [3] McGrattan, K.B, Baum, H.R. and Rehm, R.G., "Fire-Driven Flows in Enclosures", *J. Comp. Phys.* 110, No. 2, pp. 285-291, February 1994.
- [4] Baum, H.R. and Rehm, R.G., "Finite Difference Solutions for Internal Waves in Enclosures," *SIAM J. Sci. Stat. Comput.* Vol. 5, pp. 958-977, 1984.
- [5] Steckler, K.D., Baum, H.R. and Quintiere, J.G., "Fire Induced Flows through Room Openings - Flow Coefficients," Twentieth Symposium (International) on Combustion, The Combustion Institute, Pittsburgh, pp. 1591-1600, 1984.

1
2
3
4
5
6
7
8
9
10
11
12
13
14
15
16
17
18
19
20
21
22
23
24
25
26
27
28
29
30
31
32
33
34
35
36
37
38
39
40
41
42
43
44
45
46
47
48
49
50
51
52
53
54
55
56
57
58
59
60
61
62
63
64
65
66
67
68
69
70
71
72
73
74
75
76
77
78
79
80
81
82
83
84
85
86
87
88
89
90
91
92
93
94
95
96
97
98
99
100